JOURNAL OF MATERIALS SCIENCE **34** (1999) 2641–2649

Processing and thermomechanical evaluation of fibre-reinforced alumina filters

A. E. M. PAIVA, P. SEPULVEDA, V. C. PANDOLFELLI
Departamento de Engenharia de Materiais, Universidade Federal de São Carlos, Via Washington Luiz, km 235, CP 676, São Carlos–SP, 13565-905, Brazil

Impregnation of polymeric foams with ceramic suspensions has been widely employed in industry to fabricate ceramic filters of various shapes and controlled pore size at a reduced processing cost. Ceramic filters find application in cast metal industry to remove the undesired impurities from the melt, leading to products of higher quality. This paper reports a complete study on the fabrication of fibre-reinforced alumina filters. Rheological measurements of ceramic suspensions showed that the slip adherence on polymer substrate was largely improved when thickening agent was incorporated into the compositions, as a result of the increase in pseudoplasticity and in viscosity. Thermomechanical evaluation of the filters produced with fibre addition revealed that the fibre reinforcement improved the mechanical performance and reduced the damage by applied thermal stresses. Strengthening and toughening of the ceramic matrix has been explained based on the fibre properties, fibre-matrix interface strength and thermal expansion mismatch that may occur in mixed systems.

1. Introduction

Ceramic filters are critical components in the manufacture of cast metals, such as aluminium, steels and alloys. Their efficiency in removing undesired non metallic and inter-metallic inclusions from the melt can greatly improve the final quality of cast products [1]. Additionally, filters help avoid reoxidation from contact of the melt with air by reducing turbulent flow. The durability of filters depends basically on their chemical and mechanical stability when submitted to the severe conditions encountered in molten metal-slag-filter media and to the thermal and mechanical stresses characteristic of metal purification processes [2].

Among several ceramic filters processing techniques to manufacture open-celled ceramics, the impregnation of a polymeric foam with ceramic slurries has been the most widely used [3]. It allows the fabrication of bodies with a complex pore geometry and good control of pore size distribution, at a low processing cost.

1.1. Filter characteristics

Ceramic filters produced by impregnation of polymeric foams exhibit an structure which is a replica of the precursor, presenting interconnected pores (cells) of various shapes. Porous bodies can be manufactured with densities ranging from 10 to 30% of the theoretical value and differ in permeability depending on the pore shape and size, and on whether this porosity is interconnected or closed.

The selection of a raw-material for filter fabrication imposes several requirements: durability, high temperature stability, high resistance to chemical attack by molten metal, thermal shock resistance and resistance to the imposed mechanical stresses during long contact periods. Only high purity sintered ceramics are suited to the temperatures and aggressive environments involved in filtration of special metal alloys. The most commonly ceramics used include chromia or phosphate bonded alumina, cordierite, mullite, partially stabilised zirconia (PSZ), and composites of alumina-zirconia or alumina-silicon carbide [2].

Besides filter composition, pore size and its distribution can also influence the filtration efficiency. Pore size should be such to impose limits to melt flow at an acceptable pressure loss, establishing the time that melt remains in contact with filter surfaces. Porosity in the filament walls and presence of glassy phases are always undesirable in metal filtration due to their susceptibility to chemical attack.

Large inclusions present in the melt (greater than 50 μm) are trapped in the filter structure by a simple screening process. When the melt is downstream, finer pores maximise the filtration efficiency, which is governed by the adsorption rate of small impurities onto the filter surfaces [5].

The transport and attachment of small inclusions to filter wall has been described as a mechanism governed by forces and wetting angles developed from metal-inclusion-filter interactions. Non-wetting conditions (large wetting angles) in the region between liquid metal and inclusions must exist, thus the metal film between inclusion and filter wall tends to collapse and withdraw. The distance reduction leads to the development of a short range attractive force results between

inclusion and filter surface. Finally, inclusions attach permanently on the filter surface due to strong sinter bond at the operating temperature levels.

High capture efficiency is favoured by a large wetting angle of liquid metal on inclusion and by a balance between wetting angles of metal on filter. In the latter, low angles increase the efficiency of metal-filter contact, but promote greater corrosive attack of the filter when this is wetted by the alloy or slag.

1.2. Mechanical properties

Filters should withstand the thermal and mechanical stresses imposed during the process of metal purification. In this, the most critical solicitation originates from thermal shock due to the differential temperature ΔT when melt is placed in contact with the filter. A simplified expression defines the thermal stresses σ_t in rapidly cooled bodies as

$$\sigma_t = \frac{E\alpha\Delta T}{1-2\nu} \tag{1}$$

where E is the elastic modulus, α is the thermal expansion coefficient, ΔT is the thermal gradient imposed and ν is the Poisson modulus [6]. The filter ability to resist to this thermal shock will depend on the imposed conditions and on the mechanical properties of the component.

For brittle cellular structures such as those of replicated ceramic foams, the bulk properties have been described in terms of the properties of individual struts. According to Zhang and Ashby [7] the properties follow the relation

$$\text{foam property/strut properties} \propto (\rho/\rho_s)^{\frac{3}{2}} \tag{2}$$

where ρ is the foam density and ρ_s is the strut density.

This model assumes a mode of deformation which involves strut bending, and the strut strength is described as an intrinsic characteristic of the solid phase within the foam, related to the compressive strength of the foam (σ_{cr}) as

$$\sigma_{cr} = C\sigma_{fs}(\rho/\rho_s)^{\frac{3}{2}} \tag{3}$$

where σ_{fs} is the mean flexural strength of the struts, and C is a constant dependent on geometry factors estimated as 0.16 for a tetrakaidecahedral unit cell.

1.3. Fibre reinforcement

At present, the main disadvantage of replicated ceramic foams is concerned with their reduced level of fracture strength. This has been attributed to the hollow struts and flaws originated during polymer removal [8]. An approach to overcome the limited mechanical properties of replicated foams can be that of incorporating ceramic fibres as reinforcement. Fibre reinforcement in ceramics has been widely employed to avoid catastrophic failure and damage of the components induced by severe thermal stresses [9].

Fibres can enhance the strength and toughness of a ceramic matrix depending on the fibre properties and on the adhesion at the fibre-matrix interface, the latter depending on the differences in composition and thermal expansion coefficient between matrix and fibre.

Fracture of components containing fibres comprises, in general, crack formation in the matrix, crack propagation, initial failure of the reinforcement, debonding and pull-out. During these processes, the fibres tend to both limit the supply of energy to the crack tip region and to adsorb energy as the crack grows, by deflexion and twisting of the crack front. Strengthening and toughening of ceramics can be simultaneously achieved by fibre reinforcement, although a balance between the two is required, since strong fibre/matrix interfaces can produce high strength materials, while weak interfaces might favour toughening [8].

The present work is concerned with processing techniques that may lead to porous ceramics with improved mechanical characteristics. It describes the processing of alumina filters via replication of polymeric foams, employing reinforcement by fibre addition. The thermomechanical properties of filters were mesured as function of fibre content and composition. In addition, a novel technique to obtain porous ceramics is suggested, with the ability to produce compact and strong struts without the hollow part typical of replicated foams.

2. Experimental

2.1. Materials

Alumina A-3000FL (Alcoa Aluminium Company) with particle size ranging from 0.2 μm to 6 μm, and an average of approximately 3.5 μm was used as the raw-material. Sodium polyacrylate of 2500 molecular weight (Darvan 7S–Vanderbilt, USA) was used as the dispersing agent for alumina. In this work, the concentration of this substance is expressed as milligrams of polymer per grams of alumina (mg/g). A polysaccharide thickening agent (Rhone-Poulenc) was incorporated into the compositions as a means of increasing the slips' viscosity for impregnation.

High alumina fibres (Alcen B-97N, Rath Performance Fibers Inc.) and mullite fibres (Carborundum S.A.) in percentages varying from 1 to 5 wt % were tested for matrix reinforcement. The data reported in Table I describes the main characteristics of the fibre types tested.

Polyurethane foams (Reticel, UK) with pore density of 8 and 15 ppi were employed as precursors for impregnation. The temperature of polymer decomposition

TABLE I Chemical and physical properties of high alumina (Alcen B-97N) and mullite (Fibermax Bulk) fibres used as reinforcement in alumina filters

Chemical composition (wt %)	Alcen B-97N	Fibermax bulk
Al_2O_3	97.0	72.0
SiO_2	3.0	27.0
Physical properties		
Melting point (°C)	1900	1870
Average diameter (μm)	3–4	2–3.5
Average length (μm)	150	400–600
Density (g cm^{-3})	3.0–3.9	3.0

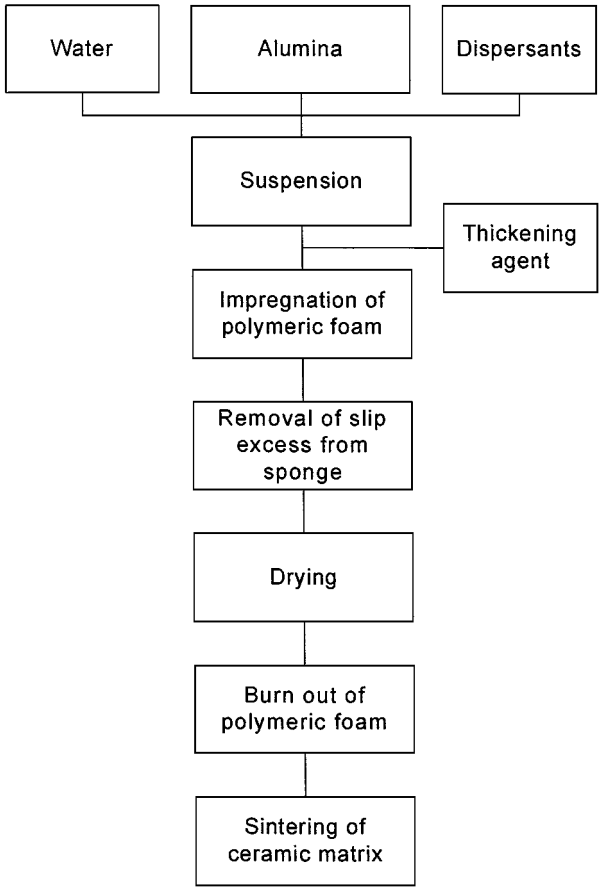

Figure 1 Flow-chart of the stages involved in filter fabrication through replication of polymeric foams.

was assessed through differential thermal analysis, at a heating rate of 1 °C/min (Netsch STA 409 thermal analysis equipment).

2.2. Procedure of filter fabrication

The steps comprised in filter fabrication via impregnation of polymeric foams is given in flow chart of Fig. 1.

2.2.1. Preparation of suspensions

Slurries were prepared containing alumina powder, deionised water and dispersants, which were thoroughly mixed to form homogeneous slips with the desired concentration of solids, 59, 73 and 82 wt %. Dispersant concentration was increased up to the point that a minimum viscosity plateau was obtained. Thickening agent was incorporated into fully dispersed suspensions in amounts of 0.16, 0.20 and 0.24 wt %. The rheological behaviour of suspensions prepared with and without thickening agent additions was evaluated using a viscometer Brookfield LVDV-III. Fibres (2–5 wt %) were included in suspensions containing solids concentration of 82 wt %, 56 mg/g of dispersant and 0.24 wt % of thickening agent.

2.2.2. Impregnation of polymeric foam

Samples of polymeric foam cut with dimensions of $50 \times 50 \times 25$ mm^3 were compressed prior to immersion into the suspensions. The impregnated sponge was passed through rollers for removal of the slip excess and elimination of closed pores. The distance between rollers was varied between 2.5 mm and 10 mm, which correspond to 10 and 40% of the sponge thickness.

Drying was carried out in oven at 100 °C for a period of 20 h. The polymeric foam and other organic material were removed from the specimens by pyrolysis in air at a heating rate of 2 °C/min to 400 °C, held for 1 h. For sintering of the ceramic matrix, samples were heated at 5 °C/min to 1600 °C and held for 3 h.

2.3. Characterisation

The filter density was calculated according to the specimen's weight and dimensions. The sponge weight was subtracted from the impregnated foam weight for the calculation of green density. Measurements of strut density were carried out by helium picnometry (Ultrapicnometer 1000 Quantachrome Co.). For this measurement, sintered foams were crushed to destroy the cellular structure and ensure a majority of single struts.

The compressive behaviour of foams was analysed on a universal machine (INSTRON 1127), at loading speed of 0.5 mm/min. A 5 mm thick rubber cap was attached to the contact surfaces of the specimens, in order to evenly distribute the loading. Due to oscillations in plots of stress versus strain, the fracture strength was averaged between the minimum and maximum peaks of stress, within the plateau range.

The specimens were submitted to a thermal shock of approximately 480 °C. They were heated at 5 °C/min up to 500 °C and held for 30 min, followed by quenching into flowing water at approximately 20 °C.

The microstructure, mainly the strut uniformity before and after thermal shock, was examined by scanning electron microscopy (SEM, ZEISS DSM 940A).

3. Results and discussions

3.1. Polymer pyrolysis

The diagrams of polyurethane thermal analyses are illustrated in Fig. 2. Polymer decomposition started at approximately 220 °C, and continued up to 480 °C in air, as revealed by the TGA curve. The DSC diagram shows, at low temperature, the loss of expansion additives used in the process of foaming. This is followed by a series of endothermic peaks that are related to the decomposition of the polymer. The degradative processes

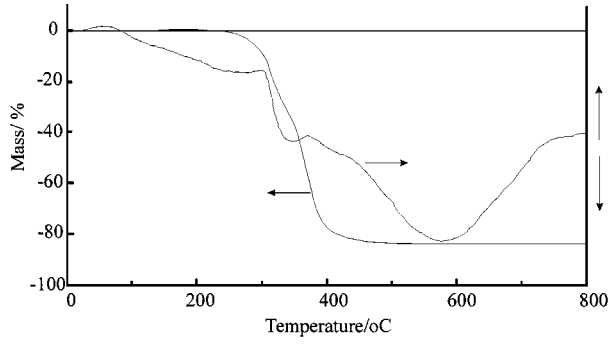

Figure 2 Differential thermal (DSC) and thermogravimetric (TGA) analyses of the polyurethane foam used as substrate in the fabrication of ceramic foams. Heating rate = 7 °C/min.

can be of different origins, depending on the structures that are broken down by chain rupture and scission.

A major fraction of polymer was eliminated between 220 and 490 °C. Thus, in this range, a control of heating rates should be essential to minimise polymer vaporisation and subsequent gas production rates. The pressure built up generated both in the microstructure and within hollow struts might exceed the strength of green struts, resulting in cracks and deterioration of filter walls. Accordingly, low heating rates are preferable during polymer removal.

Lange and Miller [4] have shown that under heating the polymer softens before decomposition, then melts and boils. During the formation of fluid polymer, little or no permeation of the liquid into the porous matrix should occur, for it would damage the ceramic matrix. High viscosity of the molten polymer is, therefore, required.

3.2. Rheology of slurries

3.2.1. Viscosity versus concentration of dispersing agents

The deflocculation curves of alumina are plotted in Fig. 3, for all compositions tested. A repulsive and a steric barrier imparted by polyelectrolytes prevent the powder from forming agglomerates and stabilise the suspensions. A minimum viscosity occurs approximately above 7, 13 and 28 mg/g of dispersant for compositions containing 58, 73 and 82 wt %, respectively. This minimum viscosity is a result of an optimum combination between polymer adsorption onto alumina particles and the polymer conformation [10].

Greater viscosity levels characterised more highly loaded slips. This has been explained on the basis that powder particles are more closely packed leading to a greater interaction on shearing. Polymer conformation assuming more stretched forms may also contribute for bridging between neighbouring particles, effect more frequently seen for dispersion using high molecular weights [11].

3.2.2. Slip rheology

Processing of fluid suspensions into consolidated bodies usually demand specific rheological characteristics.

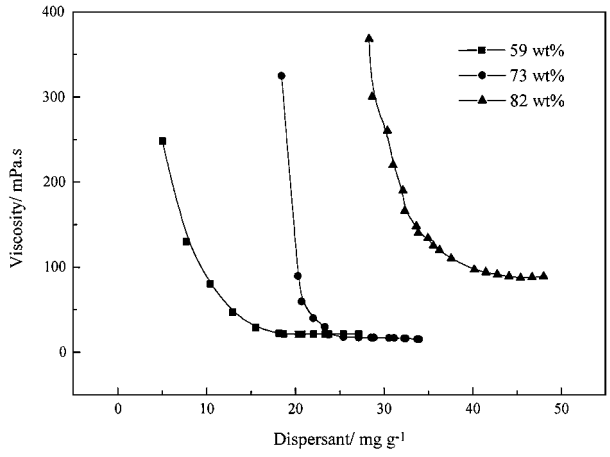

Figure 3 Viscosity against dispersant concentration, for slips containing 59, 73 and 82 wt % alumina.

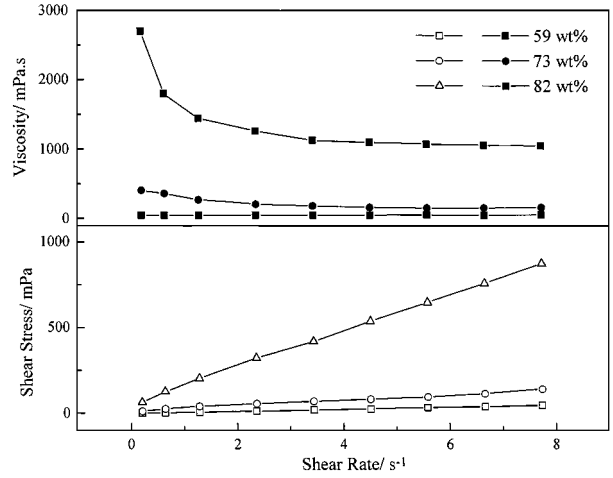

Figure 4 Shear stress and viscosity against shear rate of slips containing 59, 73 and 82 wt % alumina, dispersed at the minimum of viscosity.

For instance, in filter impregnation, slip rheology may influence the final thickness of the adhered film and posterior foam stability.

In this work, slips containing low content of solids presented a nearly Newtonian behaviour whilst pseudoplasticity characterised more highly loaded systems (see Fig. 4). Pseudoplasticity, shown by a viscosity reduction at increasing shear rate, is usually preferred for filter impregnation. This is because slip flow into the sponge is facilitated by low viscosity in the initial stages of processing, when shear forces are applied. Under static conditions, the viscosity is high preventing sedimentation and rendering high stability to slip adhered onto the polymer surface. In this manner, the foam integrity can be maintained for longer periods until drying is accomplished. An excessive pseudoplasticity is undersirable, however, because it is associated with an agglomerated state of powder particles and heterogeneous microstructures. The plots of shear stress versus shear rate show low values of yield stress, which is favourable aspect for the process of sponge impregnation when low stresses are applied.

3.2.3. Thickening agent

High viscosity and pseudoplasticity characterised compositions prepared with addition of thickening agent, as seen in plots of Fig. 5. These suspensions containing thickening agent presented a pseudoplastic behaviour, which results from the alignment of these large molecules at high shear rates [12].

The rheology of systems containing dispersant and thickening agent is determined by a competitive adsorption between these two substances onto particle surface. In general, when dispersant is first added to the slip, a strong adsorption takes place on the active sites of particles. These dispersant molecules are not easily desorbed on the addition of thickening agent. Thus, the latter tend to form inter-particle organic bridges consequently leading to an increase in the viscosity.

The polysaccharides used as thickening agent in this work are typical aiding agents employed in ceramic processing to increment the viscosity of suspensions,

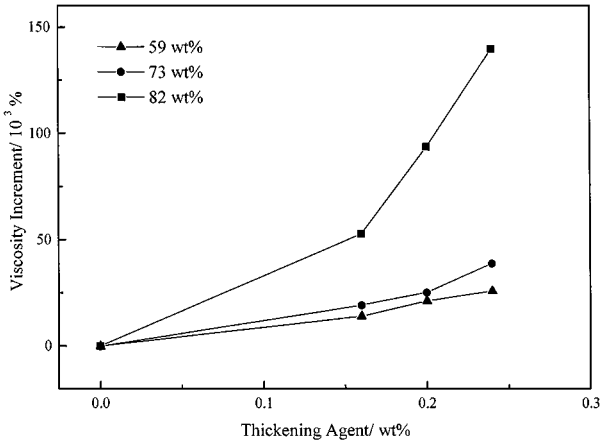

Figure 5 Effect of thickening agent concentration on the viscosity increment of alumina slips that had been previously dispersed at the minimum of viscosity. Solids loading: 59, 73 and 82 wt %. Viscosity increment is given by a perceptual ratio between the viscosity of slips prepared with and without thickening agent.

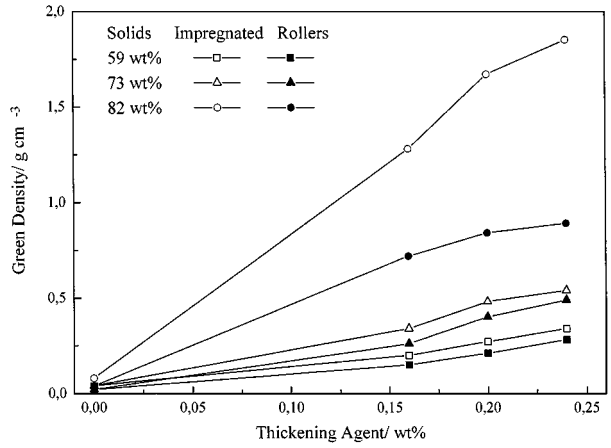

Figure 7 Effect of alumina loading and of thickening agent concentration on the final green density of 15 ppi filters. Filters were produced from uncompressed impregnated sponges (hollow symbols) and from impregnated sponges compressed at roller span of 20% (solid symbols).

and they can also impart strength to green bodies by promoting a strong inter-particle adhesion after solvent evaporation.

Alternative routes to further improve the filter processing may be the use of suspensions which include in their composition compounds that react to form gels. This would set the fluid layer adhered onto the polymer sponge yielding strength to the ceramic matrix in the green state. Substances such as cellulose derivatives [12], alginates [13] and sol-gel systems [14] could be used. The reactions that lead to gelation provide setting mechanisms to stabilise the fluid films surrounding the polymeric foam. However, problems related to timing of the gelation reactions and complex rheology of slips could appear.

3.3. Filter density

3.3.1. Effect of roller span

The diagram in Fig. 6 illustrates final green density of filters passed through rollers at various spans. Using greater spans to compress the impregnated sponge led to higher filter density and thicker filaments, nevertheless a larger number of closed pores was observed. Rollers span of 5 mm (20% of the sponge thickness) was found to be suitable for high green densities with negligible closed porosity. This condition was therefore chosen for further filter production.

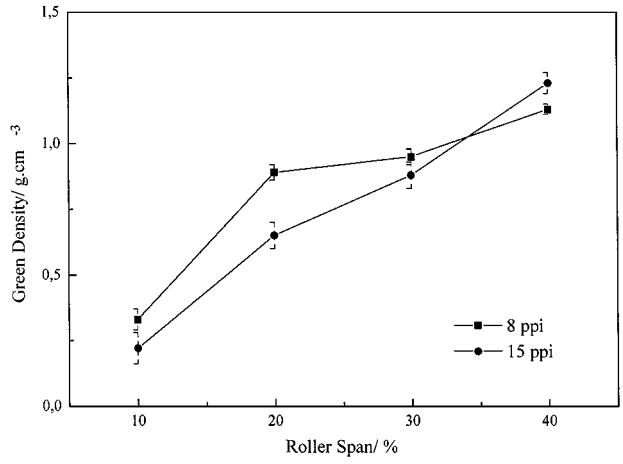

Figure 6 Effect of roller span used to compress the impregnated sponge on the green density of 8 ppi and 15 ppi filters. Span is expressed in percentage of the sponge thickness.

3.3.2. Influence of slip viscosity

The influence of thickening agent content and of slip density on the filter density is revealed in plots of Fig. 7. Slips containing higher concentration of solids and thickening agent, therefore of higher viscosity, were observed to produce more coherent coatings. The increased viscosity has an effect of preventing drainage of the fluid coating, therefore it enables the formation of thicker and more stable ceramic layers yielding denser specimens.

In metal filtration, the mechanical stresses are imposed by pressure due to incoming metal stream and to the metal head. The magnitude of these stresses can be significantly reduced by using filters with thicker struts, once the load is distributed across thicker strut diameters (stress $= P$/area). Yet, strut thickness must be increased within bounds imposed by pressure drop restrictions.

3.4. Fibre reinforced filters

An increased difficulty in impregnating sponges with slips containing fibres was found in processing, due to the reduced fluidity characteristic of these slips. This was also the reason why the fibre content had to be maintained at a maximum of 5 wt %. The filters reinforced with fibres presented final density of approximately $17\% \pm 2\%$ of the estimated theoretical one.

3.5. Mechanical properties of filters

3.5.1. Compressive failure strength

The results of filter's compressive strength are given in Fig. 8, measured before and after thermal shock.

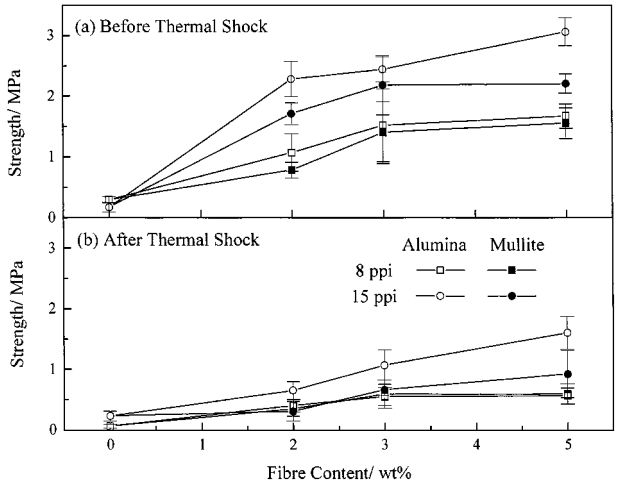

Figure 8 Effect of fibre content and composition on the compressive strength of 8 ppi and 15 ppi filters tested (a) before and (b) after the thermal shock. Filter relative density = 15%.

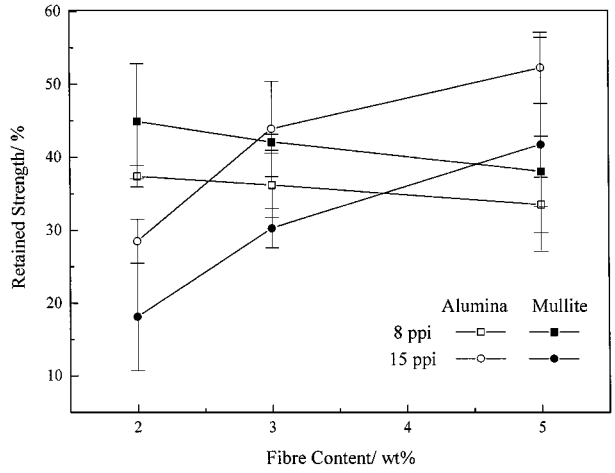

Figure 9 Effect of fibre content and composition on the retained compressive strength of (a) 15 ppi and (b) 8 ppi filters after the thermal shock. Filter relative density = 15%.

A marked influence of fibre addition on the fracture strength was detected, increasing according to the fibre content.

Despite the enhancement of mechanical properties promoted by fibres, the fracture strength of replicated foams is still extremely low, limited to values no greater than 3 MPa. This has been attributed to the presence of hollow struts and other flaws originated on polymer removal, which are intrinsic of the manufacturing process. Additionally, there exists a differential shrinkage/expansion between polymer precursor and ceramic layer adhered which have detrimental consequences on the densification of the ceramic matrix.

3.5.2. Effect of fibre composition

Table II reports the values of flexural strength calculated from Equation 3, which considers the strut compressive strength and the strut density. The estimated flexural strength presented a remarkable increase with increasing fibre concentration. Filters without reinforcement exhibited an estimated flexural strength of 17 MPa. This reached values of 175 and 255 MPa when 5 wt % of mullite and of alumina fibres were included into the compositions, respectively.

As seen, alumina fibres were more efficient in enhancing the strut strength of the alumina matrix than mullite fibres. In like-like systems, fibre and matrix tend to form strong bonds and a smooth interface, thus resulting in strong matrix-fibre interfaces and in a higher strength material. This is not a favourable condition for composite toughening, however, since a propagating crack does not feel the interface presence as well as it would do in mixed systems. Another reason for the greater increment in strut strength achieved with alumina fibres may be attributed to their superior mechanical properties compared to mullite fibres [15].

In the mullite-alumina system, the interface may have intermediate compounds or gaps owing to thermal expansion mismatch which favour crack deflection and benefit toughening. The thermal expansion mismatch between the alumina matrix and mullite fibres could have resulted in generation of defects during the manufacturing process which contributed for the lower levels of mechanical strength noted in alumina-mullite fibre filters. Still, flaws may have been generated during the process of accommodation of mullite fibres in the structure, since the average length of these fibres (400 μm) surpassed the strut diameter, and, at times, were observed to protrude out of the strut walls.

TABLE II Results of strut density measured by helium pycnometry and corresponding values of the estimated strut flexural strength for 15 ppi filters. Filter relative density = 15%

Fibre/composition	Strut density (g cm^{-3})	Flexural strength (MPa)
Without fibre	3.98 ± 0.01	17 ± 4
3 wt % alumina	3.98 ± 0.01	210 ± 4
5 wt % alumina	3.94 ± 0.01	245 ± 14
3 wt % mullite	3.93 ± 0.01	174 ± 21
5 wt % mullite	3.92 ± 0.01	175 ± 8

3.5.3. Effect of cell size

The results shown in Fig. 8 illustrate that filters of similar density but with smaller cell size exhibit greater compressive strength. This dependence of properties

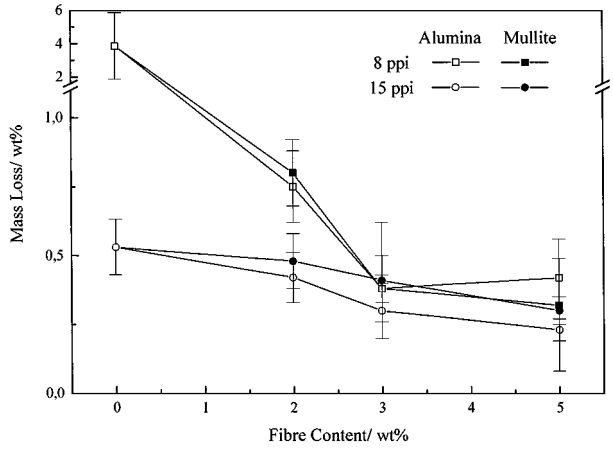

Figure 10 Effect of fibre content and composition on the mass loss of 8 and 15 ppi filters as a result of the thermal shock. Filter relative density = 15%.

(a)

(b)

Figure 11 SEM micrographs of 15 ppi filters observed (a) before and (b) after the thermal shock.

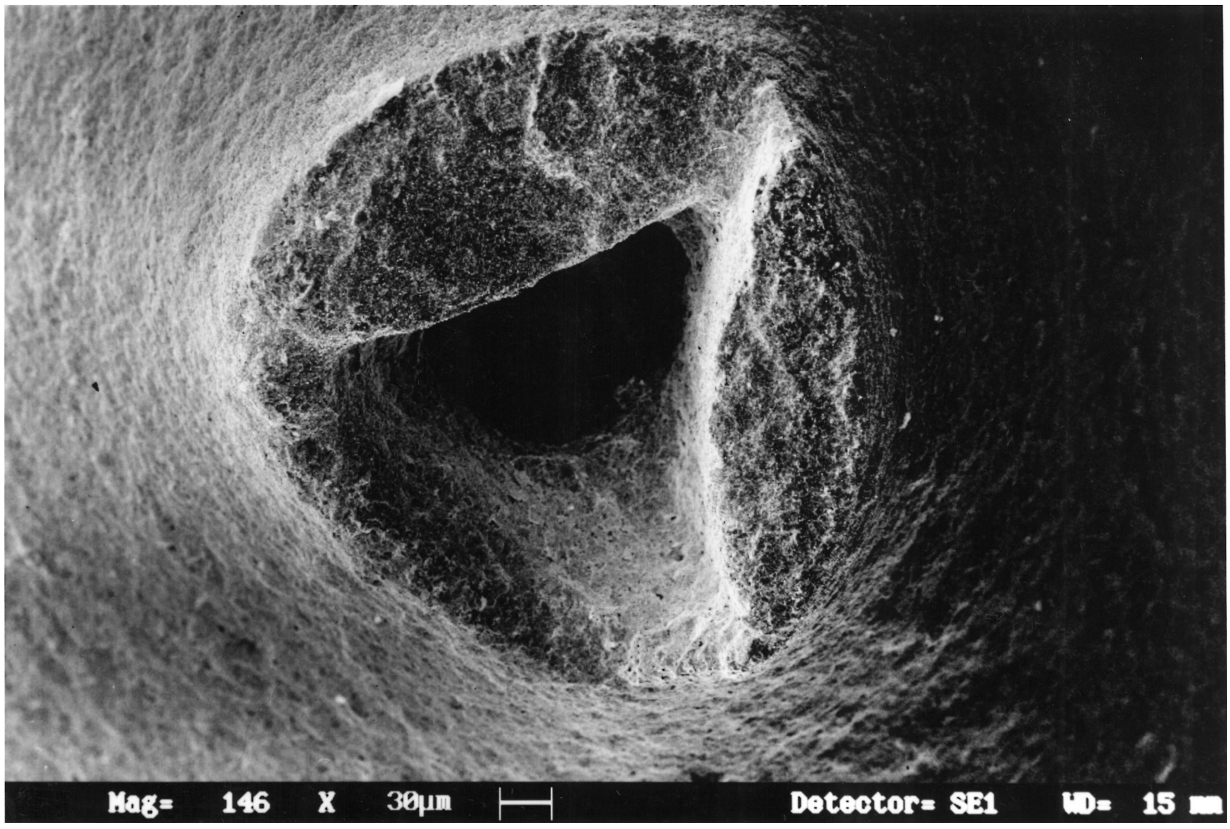

Figure 12 SEM micrograph showing the struts of cellular ceramic produced by impregnation of polymeric foam.

on cell size has not been included in models used to describe the mechanical behaviour of cellular ceramics. Brezny and Green [16] suggested that there is a dependence of strut properties on the cell size due to intrinsic characteristics of the processing route used to manufacture the filters. Thus, small cell sized-materials are usually associated with thick and even struts, which in turn, improve the mechanical properties.

3.6. Thermal shock behaviour

3.6.1. Retained compressive strength

The degradation of filter mechanical properties after thermal shock can be verified in Fig. 9. The results of retained strength demonstrate that 15 ppi filters had strength change incremented whereas 8 ppi filters presented reduced strength when fibre content was increased. This may be explained by the fact that large fibres accommodated into the thinner struts of 15 ppi filters promote greater crack arresting than that created in 8 ppi filters. This might be also the reason for the results observed in Fig. 8, of 8 ppi exhibiting slightly lower compressive strength than 15 ppi filters.

3.6.2. Mass loss

The effects of thermal shock can be also monitored by measuring the loss in the specimen mass, due to struts fragmented during quenching. The structural damage of the filter component can be related to the thermal stresses, which act on individual struts and exceed the strut failure stress. Fig. 10 shows the efficiency of fibres in minimising the filter mass loss, which appears to be smaller for increasing fibre content. This effectiveness of fibres in preventing spalling can avoid the presence of undesired particular in the molten metal and results from the toughening mechanisms mentioned earlier. Filters with 8 ppi presented greater mass loss than 15 ppi ones, confirming that the concentration of pre-existing defects is greater in 8 ppi filters. Minimum mass loss of filters during use is essential in metal purification in order to avoid the contamination of the melt with inclusions.

SEM micrographs in Fig. 11 compare the structure of a 15 ppi filter before and after the thermal shock. The microstructure in (b) illustrates how the thermal stresses can cause cracks along the strut length. The absence of macroscopic cracks propagating over several cells indicates that individual struts most probably determine the mechanical behaviour of the replicated bodies.

The micrograph in Fig. 12 illustrates a typical strut produced by replication, revealing a hollow morphology due to elimination of the polymer substrate.

4. Conclusions

Filter density of replicated foams can be conveniently varied by controlling processing parameters such as the slip viscosity and the distance between rollers used to compress the impregnated sponge. Thickening agents can be successfully employed to increase the viscosity of slips, improving slip adhesion onto polymer reticulate on impregnation and consequently producing thicker struts.

Fibre reinforcement in filters led to a significant increment in the compressive failure strength, and also

improved the thermal shock minimising the damage after thermal shock. Filters reinforced with alumina fibres presented better results than the ones produced with mullite fibres. This was attributed to the higher shear strength in fibre-matrix interfaces of like-like systems, higher mechanical properties of alumina fibres and due also to the alumina fibre size, of an order comparable to the strut diameter.

Acknowledgements

The authors would like to thank FAPESP and CAPES for the financial support to this research.

References

1. A. L. MATTHEWS, *KEY Eng. Mater.* **122** (1996) 293–303.
2. L. S. AUBREY, J. W. BROCKMEYER and M. A. MAUHAR, Fifth International Iron and Steel Congress, Proceedings of the 69th Steelmaking Conference, 1986, Chap. 119, pp. 977–991.
3. J. SAGGIO-WOYANSKY and C. E. SCOTT, *Amer. Ceram. Soc. Bull.* **11**(71) (1992) 1674–1682.
4. F. F. LANGE and K. T. MILLER, *Adv. Ceram. Mater.* **2**(4) (1987) 827–831.
5. P. F. WIESER, Fifth International Iron and Steel Congress, Proceedings of the 69th Steelmaking Conference, 1986, Chap. 119, pp. 969–976.
6. R. M. ORENSTEIN and D. J. GREEN, *J. Amer. Ceram. Soc.* **75**(7) (1992) 1899–1905.
7. J. ZHANG and M. F. ASHBY, "Theoretical Studies on Isotropic Foams" (Cambridge University Publication no. CUED/C-MATS/TR 158, Cambridge University, Cambridge, UK, 1989).
8. R. W. DAVIDGE, *Composites* **18**(2) (1987) 92–98.
9. H. WANG and R. N. SINGH, *Int. Mater. Rev.* **39**(6) (1994) 228–244.
10. J. CESARANO and I. A. AKSAY, *J. Amer. Ceram. Soc.* **71**(4) (1988) 250–255.
11. F. S. ORTEGA, P. SEPULVEDA, M. YOSHISAWA, E. FROLLINI and V. C. PANDOLFELLI, *Anais da Associação Brasileria de Química*, in press.
12. R. MORENO, *Amer. Ceram. Soc. Bull.* **11**(71) (1992) 1647–1657.
13. H. KATSUKI, A. KAWAHARA and H. ICHINOSE, *J. Mater. Sci.* **27** (1992) 6067–6070.
14. D. A. HIRSCHFELD, T. K. LI and D. M. LIU, *KEY Eng. Mater.* **115** (1996) 65–80.
15. M. H. STACEY, *Brit. Ceram. Trans. J.* (87) (1988) 168–172.
16. R. BREZNY and D. J. GREEN, *J. Amer. Ceram. Soc.* **72**(7) (1989) 1145–1152.

Received 25 October 1997
and accepted 8 October 1998